Acta Cryst. (1986). A42, 414-426

Angular Dependence of the Absorption-Induced Nodal Plane Shifts of X-ray Stationary Waves

BY A. AUTHIER

Laboratoire de Minéralogie-Cristallographie, Universités Paris 6 et 7, associé au CNRS, 4 Place Jussieu, 75252 Paris CEDEX 05, France

(*Received* 17 *December* 1985; *accepted* 24 *February* 1986)

Abstract

The classical equations of dynamical theory in the Bragg case are rederived in a way which is valid even in the presence of absorption where every quantity used is complex. The properties of the phase and the amplitude of the diffracted wave are discussed in detail. It is shown that for non-centrosymmetric crystals the position of the nodes at the centre of the reflection domain is strongly absorption dependent. The limit of the phase of the ratio of the diffracted to the incident amplitude far from the reflection domain is calculated to be equal to $\varphi_h + \pi$ and φ_h, below and above the reflection domain, respectively, where φ_h is the phase of the structure factor calculated taking into account anomalous dispersion and the imaginary part of the form factor. It is therefore absorption dependent and so is the position of the nodes of stationary waves which is never invariant with the angular position of the crystal, even outside the total reflection domain. The example of a non-centrosymmetric crystal, GaAs, opposite reflections, 111 and $\bar{1}\bar{1}\bar{1}$, and of wavelengths close to the absorption edges of gallium and arsenic is used to illustrate the results. It shows that the absorption-induced shifts of the nodal planes are in general directed towards the surface of the crystal, independently of the sense of the diffraction vector. The variation of the penetration depth within the total reflection is interpreted in the non-absorbing case by means of a new surface which completes the dispersion surface within the Bragg gap.

1. Introduction

At Bragg total reflection, the incident, $\mathbf{K}_0$, and reflected, $\mathbf{K}_h$, waves interfere generating a set of stationary waves which are hooked to the bulk of the crystal and extend through the surface towards the outside. Atoms situated at the antinodes of electric field emit fluorescent X-rays and electrons whose energy is characteristic of their nature. The nodes and antinodes lie on planes parallel to the diffracting planes whose spacing d is the lattice spacing divided by the order of the reflection. When the crystal is rocked through the reflection domain, the nodes and antinodes move towards the inside of the crystal by $d/2$. The simultaneous recording of the emitted fluorescent X-rays in a multichannel analyser and of the rocking curve enable the positions of the atoms within the unit cell to be determined to a few percent. This technique was first proposed by Batterman (1964, 1969) and is currently used by several groups to study the structure of surfaces and interfaces (see, for instance, Kruglov, Sozontov, Shchemelev & Zhakarov, 1977; Takahashi & Kikuta, 1979; Golovchenko, Patel, Kaplan, Cowan & Bedzyk, 1982; Patel & Golovchenko, 1983; Bedzyk, Materlik & Kovalchuk, 1984; Bedzyk & Materlik, 1985*a*, *b*; Patel, Golovchenko, Bean & Morris, 1985; Durbin, Berman, Batterman & Blakeley, 1986; Afanas'yef, Imamov, Maslov & Paishayev, 1985). Its principle is based on the knowledge of the positions of the system of stationary waves.

In non-absorbing crystals, three cases can be distinguished: on the small-angle side of the total reflection domain, the nodes lie on the planes along which the Fourier component of the electronic density is maximum. On the other side, they lie halfway between these planes. Within the total reflection domain, the nodes move progressively from one position to the other. In absorbing crystals, however, the position of the nodes varies continuously even outside the total reflection domain and it is therefore very important to include correctly the effect of absorption.

The notion and the basic properties of wave fields were introduced by Ewald (1917, 1927) and the form of the dynamical theory which is used today was developed by von Laue (1931) after Ewald. Its main results and modern developments are to be found in various books and reviews such as Zachariasen (1945), von Laue (1960), James (1963), Batterman & Cole (1964), Kato (1974), Pinsker (1978), and Authier (1961, 1970).

The aim of this paper is to rederive the basic equations of dynamical theory diffraction by perfect crystals in a way which is rigorous even in the presence of strong absorption and to discuss the variation of the phase and the amplitude of the diffracted wave in the Bragg case with a view to determining the influence of absorption on the exact position of the nodes of standing waves (Authier, 1985). A geometric interpretation of the variation of the penetration depth within the total reflection range for a non-absorbing crystal will also be given.

0108-7673/86/060414-13$01.50

2. Fourier components of the dielectric susceptibility

We shall call χ_h, χ_{rh}, χ_{ih} the Fourier components of the dielectric susceptibility and its real and imaginary parts, respectively:

$$\chi_h = \chi_{rh} + i\chi_{ih} = -|\chi_h| \exp i\varphi_h. \tag{2.1}$$

They are related to the structure factor through the relations

$$\begin{cases} \chi_h = -(R\lambda^2/\pi V)F_h = -(R\lambda^2/\pi V)|F_h| \exp i\varphi_h \\ \chi_{rh} = -(R\lambda^2/\pi V)F_{rh} = -(R\lambda^2/\pi V)|F_{rh}| \exp i\varphi_{rh} \\ \chi_{ih} = -(R\lambda^2/\pi V)F_{ih} = -(R\lambda^2/\pi V)|F_{ih}| \exp i\varphi_{ih}, \end{cases} \tag{2.2}$$

where R is the classical radius of the electron, λ the wavelength, V the volume of the unit cell and

$$\begin{cases} F_{rh} = \sum (f_j + f_j') \exp - M_j \exp -2\pi i\mathbf{h} \cdot \mathbf{r}_j \\ F_{ih} = \sum f_j'' \exp - M_j \exp -2\pi i\mathbf{h} \cdot \mathbf{r}_j, \end{cases} \tag{2.3}$$

f_j is the form factor of atom j, f_j' the anomalous dispersion correction, f_j'' its imaginary part and $\exp -M_j$ the Debye-Waller factor.

The Fourier component corresponding to the $\bar{h}\bar{k}\bar{l}$ reflection is

$$\chi_{\bar{h}} = \chi_{rh}^* + i\chi_{ih}^*, \tag{2.4}$$

where the star means complex conjugate (hence $\chi_{\mathbf{h}} \neq \chi_{\mathbf{h}}^*$).

We shall set

$$\begin{cases} \varphi = \varphi_{rh} - \varphi_{ih}; \quad \kappa = |\chi_{ih}/\chi_{rh}| = |F_{ih}/F_{rh}| \\ (\chi_h\chi_{\bar{h}})^{1/2} = |\chi_h\chi_{\bar{h}}|^{1/2} \exp i\beta \\ \sigma^{1/2} = (\chi_h\chi_{\bar{h}})^{1/2}/\chi_{\bar{h}} = -|\sigma|^{1/2} \exp i\beta', \end{cases} \tag{2.5}$$

where the modulus of $\sigma = \chi_h/\chi_{\bar{h}}$ is the departure from Friedel's law in absorbing crystals, that is the ratio of the intensities of the hkl and $\bar{h}\bar{k}\bar{l}$ reflections, respectively. The ratio κ has the same meaning as in Zachariasen (1945). These quantities are frequently used in dynamical theory as will be seen later and it can be shown that

$$\begin{cases} |\sigma| = [(1 + 2\kappa \sin\varphi + \kappa^2)/(1 - 2\kappa \sin\varphi + \kappa^2)]^{1/2} \\ \beta + \beta' = \varphi_h. \end{cases} \tag{2.6}$$

Phase angle β does not depend on the position of the origin of the unit cell and is small in general while β' depends on this origin. To a very good approximation, even close to an absorption edge,

$$\begin{cases} |\chi_h\chi_{\bar{h}}| \simeq |\chi_{rh}|^2(1 + \kappa^2 \cos 2\varphi) \\ \beta \simeq \kappa \cos\varphi/(1 - \kappa^2 \sin^2\varphi) \\ \beta' \simeq \varphi_{rh} - \beta\kappa \sin\varphi. \end{cases} \tag{2.7}$$

Far from an absorption edge, we have

$$|\sigma| \simeq 1 + 2\kappa \sin\varphi. \tag{2.8}$$

In a centrosymmetric crystal:

$$\varphi = 0 \text{ or } \pi; \quad \beta = \pm\kappa; \quad \beta' = \varphi_{rh}; \quad |\sigma| = 1. \tag{2.9}$$

If the origin of the unit cell is situated at a centre of symmetry, $\beta' = 0$.

3. Fundamental equations of two-wave dynamical theory in the absorbing case

Dynamical theory provides a solution of the propagation equation of a wave in a periodic medium. In the two-beam approximation the solution is a wave field:

$$\mathbf{D} = \exp -2\pi i\mathbf{K}_0 \cdot \mathbf{r}(\mathbf{D}_0 + \mathbf{D}_\mathbf{h} \exp 2\pi i\mathbf{h} \cdot \mathbf{r}), \tag{3.1}$$

where $\mathbf{h}$ is the reciprocal-lattice vector associated with the reflection. It can also be written:

$$\mathbf{D} = \mathbf{D}_0 \exp -2\pi i\mathbf{K}_0 \cdot \mathbf{r} + \mathbf{D}_\mathbf{h} \exp -2\pi i\mathbf{K}_\mathbf{h} \cdot \mathbf{r}. \tag{3.2}$$

It is interpreted as the superposition of two plane waves with amplitudes $\mathbf{D}_0$ and $\mathbf{D}_\mathbf{h}$, respectively, and wave vectors $\mathbf{K}_0$ and $\mathbf{K}_\mathbf{h}$ related by

$$\mathbf{K}_\mathbf{h} = \mathbf{K}_0 - \mathbf{h}. \tag{3.3}$$

In the absorbing case, both the amplitudes and the wave vectors are complex. They satisfy a set of linear equations derived from the propagation equation on one hand and the boundary conditions at the crystal surfaces on the other. The set of linear equations is

$$\begin{cases} 2X_0D_0 - kC\chi_{\bar{h}}D_h = 0 \\ -kC\chi_hD_0 + 2X_hD_h = 0 \end{cases} \tag{3.4}$$

with

$$\begin{cases} X_0 = [K_0^2 - k^2(1 + \chi_0)]/2k \\ X_h = [K_h^2 - k^2(1 + \chi_0)]/2k. \end{cases} \tag{3.5}$$

$C = 1$ or $\cos 2\theta$, depending on whether the polarization is normal or parallel to the plane of incidence.

The set of equations (3.4) has a non-trivial solution if the corresponding secular equation is satisfied:

$$X_0X_h = k^2C^2\chi_h\chi_{\bar{h}}/4. \tag{3.6}$$

Following the notation of Penning & Polder (1961) we shall call ξ the ratio between the amplitudes of the reflected and incident waves. From (3.5), it is

$$\xi = D_h/D_0 = 2X_0/(kC\chi_{\bar{h}}). \tag{3.7}$$

There are two boundary conditions. The first is the continuity of the tangential components of the wave vectors on the crystal surface, the second the continuity of the electric displacement.

Let us consider the first condition and let $\mathbf{K}_0^{(a)} = \mathbf{0M}$ be the incident wave vector (Fig. 1*b*). Let us further set

$$\mathbf{K}_0 = \mathbf{0P}; \qquad \mathbf{K}_\mathbf{h} = \mathbf{HP}.$$

The extremity P of the wave vector inside the crystal

is called the *tie point*. The convention used for the orientation of the wave vectors is at the origin of that used for writing Bragg's law (3.3). The tie point is imaginary for an absorbing crystal and within the total reflection domain for a non-absorbing crystal. We shall therefore set

$$\mathbf{K}_0 = \mathbf{K}_{0r} + i\mathbf{K}_{0i}. \tag{3.8}$$

The continuity of the tangential component of the wave vectors across the crystal surface can be written

$$\mathbf{K}_0^{(a)} - \mathbf{K}_0 = \mathbf{0M} - \mathbf{0P} = \mathbf{PM} = \overline{PM}\,\mathbf{n}, \tag{3.9}$$

where $\mathbf{n}$ is the normal to the crystal surface, oriented towards the inside of the crystal. From (3.9) and (3.3) we deduce that only the projections of $\mathbf{K}_0$ and $\mathbf{K}_h$ on the normal to the crystal surface have an imaginary part and that these imaginary parts are equal:

$$\mathbf{K}_{0i} = \mathbf{K}_{hi} = \mathrm{Im}\,(\overline{MP})\mathbf{n}. \tag{3.10}$$

The square of the amplitude of the wave vector, K_0^2, (3.8), is

$$K_0^2 = K_{0r}^2 - K_{0i}^2 + 2i\mathbf{K}_{0r} \cdot \mathbf{K}_{0i}. \tag{3.11}$$

Let γ_0 be the cosine of the angle Ψ_0 between the normal to the crystal surface and the incident direction (Fig. 1*a*). The expression for K_0^2 can therefore be written

$$K_0^2 = K_{0r}^2 - K_{0i}^2 + 2i\gamma_0 K_{0r} K_{0i}. \tag{3.12}$$

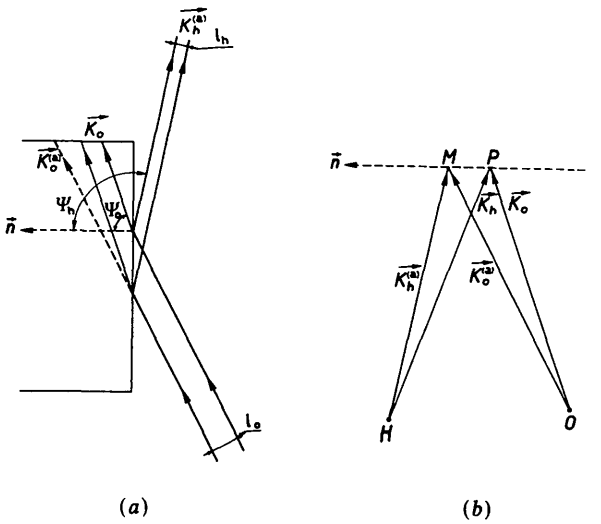

(*a*) (*b*)

Fig. 1. Incident and reflected wave vectors in direct and reciprocal space in the Bragg case. $\mathbf{K}_0^{(a)} = \mathbf{0M}$, $\mathbf{K}_h^{(a)} = \mathbf{HM}$: incident and reflected waves outside the crystal; $\mathbf{K}_0 = \mathbf{0P}$, $\mathbf{K}_h = \mathbf{HP}$: incident and reflected waves inside the crystal; $\mathbf{n}$: normal to the crystal surface. (*a*) Direct space: l_0 and l_h are the cross sections of the direct and reflected beams, respectively: $l_0/l_h = |\cos \Psi_h|/\cos \Psi_0 = |\gamma|$. (*b*) Reciprocal space: according to the boundary condition of the continuity of the tangential component of the wave vector the extremities P of $\mathbf{K}_0$ and M of $\mathbf{K}_0^{(a)}$ lie on the normal $\mathbf{n}$ to the crystal surface.

The absolute values of X_0 and X_h are always of the order of the wave number in vacuum, k, multiplied by the electric susceptibility, $|\chi|$, which is very small ($\sim 10^{-5}$), and are therefore also small. This is also true of K_{0i}, even close to an absorption edge or within the total reflection domain while K_{0r} is of the order of k. From (3.5) and (3.12) it can then be deduced, very easily for X_{0i} and after some calculations for X_{0r}, that, to a good approximation,

$$\begin{cases} X_{0r} = K_{0r} - k(1 + \chi_{r0}/2) \\ X_{0i} = \gamma_0 K_{0i} - k\chi_{i0}/2. \end{cases} \tag{3.13}$$

In the derivation given in the next section, the complex value of X_0 will be determined directly and the value of K_{0i} will be calculated through (3.13).

The intensity of the wave field $\mathbf{D}$ (3.1) can now be written

$$|D|^2 = \exp -(z/z_0)|D_0|^2[1 + |\xi|^2 + 2|\xi| C \cos(2\pi \mathbf{h} \cdot \mathbf{r} + \psi)], \tag{3.14}$$

where ψ is the phase angle of ξ, z the depth within the crystal and

$$z_0 = -(4\pi K_{0i})^{-1} \tag{3.15}$$

is the penetration depth. The absorption coefficient along the incident direction, μ, is

$$\begin{aligned} \mu &= \gamma_0 / z_0 = -4\pi K_{0i}\gamma_0 \\ &= -2\pi k\chi_{i0} - 4\pi X_{0i}. \end{aligned} \tag{3.16}$$

The first term is the normal absorption coefficient, μ_0, and (3.16) can be written

$$\mu = \mu_0 - 4\pi X_{0i}. \tag{3.17}$$

The second term in the expression for μ depends both on the photoelectric absorption and on extinction: it is equal to zero far from the Bragg condition and, within the total reflection domain, is the extinction coefficient for a non-absorbing crystal.

Equation (3.14) shows that the interference between the incident and the reflected waves is at the origin of the stationary waves. It is well known that $\mathbf{h} \cdot \mathbf{r} =$ constant is the equation of a family of planes in direct space whose spacing d is the lattice spacing divided by the order of the reflection. The product $\mathbf{h} \cdot \mathbf{r}$ can therefore be written

$$\mathbf{h} \cdot \mathbf{r} = N + \Delta d/d, \tag{3.18}$$

where Δd is the distance from the origin of the unit cell along the normal to the reflecting planes oriented towards the inside of the crystal and N is an integer.

The nodes and antinodes have a periodicity equal to d and the position of the antinodes in the unit cell is given by

$$\Delta d/d = N - \psi/2\pi. \tag{3.19}$$

4. Solution of the fundamental equations of dynamical theory

4.1. *Coordinates of the tie point*

The aim of this section is to determine the tie point from the values of X_0 and X_h which have simple geometric interpretations in the non-absorbing case only; they will be discussed in § 5. The derivation in the present section is valid even in the case of an absorbing crystal.

Let us consider the usual construction in reciprocal space where the Laue point L_a is the intersection of the two spheres of radii $k=1/\lambda$ and centred at the reciprocal-lattice points 0 and H with the plane of incidence. These spheres are approximated by their tangential planes. Let T_0' and T_h' be their intersections with the plane of incidence, respectively (Fig. 2). The extremity of the incident wave vector $\mathbf{0M}=\mathbf{K}_0^{(a)}$ lies on T_0'. In an absorbing crystal, the wave vectors inside the crystal, $\mathbf{K_0}=\mathbf{0P}$ and $\mathbf{K_h}=\mathbf{HP}$ are complex. One can nevertheless write

$$\begin{cases}\mathbf{K_0}=\mathbf{0P}=\mathbf{0L_a}+\mathbf{L_aM}+\mathbf{MP}\\ \mathbf{K_h}=\mathbf{HP}=\mathbf{HL_a}+\mathbf{L_aM}+\mathbf{MP},\end{cases}\tag{4.1}$$

where $\mathbf{MP}$ is complex.

We shall set

$$\overline{L_aM}=k\,\Delta\theta,$$

where $\Delta\theta$ is the departure from Bragg incidence of the incident wave, oriented in such a way that it is positive when the angle of incidence is larger than the Bragg angle (Fig. 2).

From (4.1), (3.5) and (3.12) and a similar equation for K_h^2, we get, neglecting high-order terms,

$$\begin{cases}X_0=\gamma_0\overline{MP}-k\chi_0/2\\ X_h=\gamma_h\overline{MP}-k\,\Delta\theta\sin 2\theta-k\chi_0/2,\end{cases}\tag{4.2}$$

where γ_h is the cosine of the angle Ψ_h between the normal to the crystal surface and the reflected wave vector (Fig. 1*b*). It is negative in the Bragg case, positive in the Laue case.

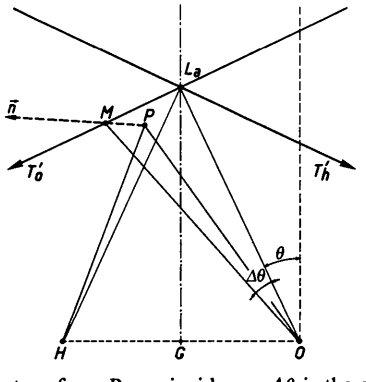

Fig. 2. Departure from Bragg incidence. $\Delta\theta$ is the angle between the wave vector satisfying Bragg's geometric condition and the incident wave vector $\mathbf{K}_0^{(a)}=\mathbf{0M}$. θ is the geometric Bragg angle. GL_a, normal to the reciprocal-lattice vector, is parallel to the reflecting planes.

Equations (4.2) can be combined and written:

$$\begin{aligned}\overline{MP}&=X_0/\gamma_0+k\chi_0/2\gamma_0\\&=X_h/\gamma_h+k\chi_0/2\gamma_h+k\,\Delta\theta\sin 2\theta/\gamma_h.\end{aligned}\tag{4.3}$$

We shall set

$$\begin{aligned}\eta&=[\Delta\theta\sin 2\theta+\chi_0(1-\gamma)/2]\\&\quad\times[|C|(\chi_h\chi_{\bar h}|\gamma|)^{1/2}]^{-1}\\&=\text{deviation parameter}\\ \Lambda&=\lambda(\gamma_0|\gamma_h|)^{1/2}[|C|(\chi_h\chi_{\bar h})^{1/2}]^{-1}\\&=\text{extinction distance},\end{aligned}\tag{4.4}$$

where $\gamma=\gamma_h/\gamma_0$ and the definition of the deviation parameter η is after Authier (1961).

With these relations, (3.6) and (4.3) can be rewritten:

$$\begin{cases}(X_0/\gamma_0)(X_h/\gamma_h)=S(\gamma_h)/4\Lambda^2\\ X_0/\gamma_0-X_h/\gamma_h=\eta S(\gamma_h)/\Lambda,\end{cases}\tag{4.5}$$

where $S(F)$ means sign of F.

The solutions of (4.5) are

$$\begin{cases}X_0=\gamma_0S(\gamma_h)\{\eta\pm[\eta^2+S(\gamma_h)]^{1/2}\}/2\Lambda\\ X_h=\gamma_hS(\gamma_h)[-\eta\pm[\eta^2+S(\gamma_h)]^{1/2}\}/2\Lambda\end{cases}\tag{4.6}$$

and the expression for the ratio of the amplitudes of the two waves in the wave field is

$$\xi=\sigma^{1/2}S(\gamma_h)S(C)[\eta\pm[\eta^2+S(\gamma_h)]^{1/2}\}/|\gamma|^{1/2}.\tag{4.7}$$

In the Bragg case, as has been mentioned before, $S(\gamma_h)$ is negative. We shall set

$$\begin{cases}\eta^2-1=\rho^2\exp 2i\omega\\ \eta\pm(\eta^2-1)^{1/2}=Z\exp i\psi'=\eta+\rho\exp i\omega,\end{cases}\tag{4.8}$$

where there are two solutions, ω' and $\omega'+\pi$, the proper value being that for which Z and $|\xi|$ do not diverge far from the reflection domain.

Using (2.5) and (4.8), (4.6) and (4.7) can be written in the Bragg case:

$$\begin{cases}X_0=-\gamma_0Z(\exp i\psi')/2\Lambda\\ \quad=-k|C|Z|\chi_h\chi_{\bar h}|^{1/2}[\exp i(\beta+\psi')]/2|\gamma|^{1/2}\\ X_h=\gamma_hZ^{-1}(\exp -i\psi')/2\Lambda\\ \quad=-k|C|Z^{-1}|\chi_h\chi_{\bar h}\gamma|^{1/2}[\exp i(\beta-\psi')]/2\\ \xi=S(C)|\sigma|^{1/2}Z[\exp i(\beta'+\psi')]/|\gamma|^{1/2}.\end{cases}\tag{4.9}$$

Equations (4.9), (4.8), (4.4) and (2.5) show that the phase angle ψ of ξ, introduced in (3.14), is

$$\psi=\beta'+\psi'\tag{4.10}$$

when θ is smaller than 45° or for $C=1$.

4.2. *Reflecting power*

This paper will be limited to the Bragg case for a thick crystal. In that case, one wave field only is excited in the crystal, that which propagates towards the inside of the crystal, the other one propagating outwards from the inside towards the surface being absorbed. The appropriate wave field is also that whose intensity tends towards zero far from the reflecting domain, as mentioned above. The value of the amplitude, $\mathbf{D}_h^{(a)}$, of the reflected wave outside the crystal is obtained by applying the boundary conditions which are particularly simple in this case:

$$\mathbf{D}_0 = \mathbf{D}_0^{(a)}; \quad \mathbf{D}_h^{(a)} = \mathbf{D}_h. \tag{4.11}$$

The reflecting power is equal to the ratio of the reflected to the incident energies and therefore to the product of the ratio $|\xi|^2$ of the reflected intensity to that of the incident wave by the ratio $|\gamma|$ of the cross sections of the reflected and incident beams, respectively (Fig. 1). From (4.9) it becomes

$$I_h = |\gamma|\,|\xi|^2 = |\sigma| Z^2. \tag{4.12}$$

5. Solution in the non-absorbing Bragg case

5.1. *Coordinates of the tie point*

The wave vectors are real and a geometrical interpretation can be found for all the parameters used. The quantities X_0 and X_h defined by (3.5) can be written, outside the total reflection domain, to a very good approximation,

$$\begin{cases} X_0 = K_0 - k(1+\chi_0/2) \\ X_h = K_h - k(1+\chi_0/2). \end{cases} \tag{5.1}$$

Let us consider the spheres centred at 0 and H in reciprocal space with radii $nk = k(1+\chi_0/2)$, the wave number inside the crystal. Equation (5.1) shows that X_0 and X_h are to be interpreted as the distances of the tie point from these two spheres. The secular equation (3.6) means that the product of these distances is constant. It is the equation of the locus of the tie point, that is, the dispersion surface. The spheres of radius nk can be approximated by their tangential planes. Let T_0 and T_h be the intersections of these planes with the $\mathbf{K_0}$, $\mathbf{K_h}$ planes, respectively. The cross point of these two lines is called the Lorentz point, L_0. The intersection of the dispersion surface with this plane is a hyperbola with T_0 and T_h as asymptotes (Fig. 3). The angle between these asymptotes is 2θ and the diameter of the dispersion surface is

$$\Lambda_0^{-1} = k|C|(\chi_h \chi_{\bar{h}})^{1/2}/\cos\theta. \tag{5.2}$$

Let us set

$$\begin{cases} \Delta\theta_0 = -\chi_0(1-\gamma)/2\sin 2\theta \\ \delta = 2\lambda|\gamma_h|/\Lambda \sin 2\theta. \end{cases} \tag{5.3}$$

The expressions for the deviation parameter η and for ξ, defined by (4.4) and (4.9), respectively, can now be written:

$$\begin{cases} \eta = 2(\Delta\theta - \Delta\theta_0)/\delta \\ \xi = S(C)Z[\exp i(\varphi_h + \psi')]/|\gamma|^{1/2}. \end{cases} \tag{5.4}$$

The phase angle of ξ, ψ, given by (4.10) in the general case, reduces to

$$\psi = \varphi_h + \psi', \tag{5.5}$$

where, as defined in (2.2), φ_h is the phase angle of the structure factor.

5.2. *Geometrical interpretation*

Fig. 3(a) shows the dispersion surface and the geometrical construction of the tie point. From the extremity, M, of the incident wave vector, one draws the normal to the crystal surface, $\mathbf{n}$. It intersects the dispersion surface at either real or imaginary points. The latter situation corresponds to the total reflection domain. Let I_1 and I_2 (Fig. 3a) be the points of the dispersion surface where the tangent is parallel to $\mathbf{n}$, I_{01}, I_{h1}, I' the intersections of the tangent at I_1 with T_0, T_h, T'_0, respectively, I_{02}, I_{h2}, I'' the intersections of the tangent at I_2 with the same lines, I the intersection of the parallel to $\mathbf{n}$ drawn from the Lorentz point with T'_0. The geometrical interpretations of the

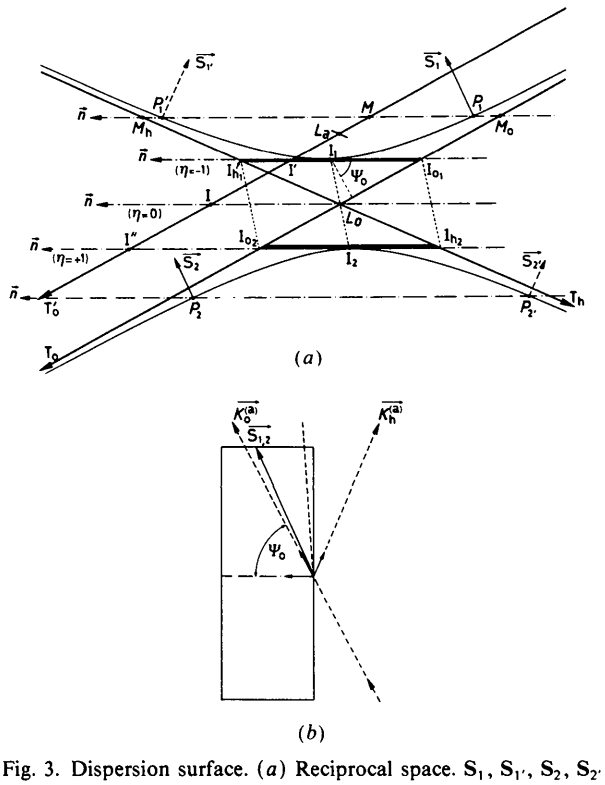

Fig. 3. Dispersion surface. (a) Reciprocal space. S_1, $S_{1'}$, S_2, $S_{2'}$ represent the Poynting vectors (propagation vectors) at P_1, $P_{1'}$, P_2, $P_{2'}$, respectively. (b) Direct space.

quantities defined in (4.4) and (5.3) are, respectively,

$$\begin{cases} \Lambda^{-1} = \overline{I_{01} I_{h1}} \\ \Delta\theta_0 = \overline{L_a I}/k = \text{angle between the middle of the reflection domain and the geometrical Bragg angle} \\ \delta = \overline{I' I''}/k = \text{width of the total reflection domain.} \end{cases} \tag{5.6}$$

Let M_0 and M_h be the intersections of the normal to the crystal surface drawn from M with T_0 and T_h, respectively; its intersections with the dispersion surface belong to the same branch when they are real. Let them be P_1 and P_1' for branch 1 (that on the same side as the Laue point) and P_2 and P_2' for branch 2. It is a well established fact in dynamical theory that the propagation direction of a wave field is given by that of the normal to the dispersion surface at its tie point. A comparison of Fig. 3(a) drawn in reciprocal space and Fig. 3(b) drawn in direct space shows that at tie points P_1 and P_2 the excited wave fields propagate towards the inside of the crystal, while those excited at P_1' and P_2' would propagate towards the outside of the crystal. In a semiinfinite or a very thick crystal, only the wave fields propagating towards the inside are actually excited since the other ones would be absorbed out before reaching the crystal surface.

The geometrical interpretation of η and $(\eta^2-1)^{1/2}$ are, respectively,

$$\begin{cases} \eta = -\overline{M_0 M_h}/\overline{I_{01} I_{h1}} \\ (\eta^2-1)^{1/2} = \overline{P_1 P_1'}/\overline{I_{01} I_{h1}}. \end{cases} \tag{5.7}$$

In other words, $\eta = -1$ when M is at I' and $\eta = +1$ when M is at I'' (Fig. 3).

5.3. *Variation of the phase of the reflected wave*

When $|\eta| > 1$, the phases ω and ψ' defined in (4.8) are constant. The condition that $|\xi|$ should tend towards zero when $\eta \to \pm\infty$ shows that they are equal to 0 and π for $\eta \leq -1$ and to π and 0 for $\eta \geq 1$, respectively. For $|\eta| \leq 1$, we have, by continuity,

$$\psi' = \tan^{-1}[(1-\eta^2)^{1/2}/\eta]. \tag{5.8}$$

The values of X_0 and Z in the three parts of the reflection domain are therefore

$$\begin{cases} \eta \leq -1: & X_0 = -\gamma_0[\eta + (\eta^2-1)^{1/2}]/2\Lambda; \\ & Z = -[\eta + (\eta^2-1)^{1/2}]; \\ -1 \leq \eta \leq -1: & X_0 = -\gamma_0[\eta + i(1-\eta^2)^{1/2}]/2\Lambda; \\ & Z = 1; \\ \eta \geq -1: & X_0 = -\gamma_0[\eta - (\eta^2-1)^{1/2}]/2\Lambda; \\ & Z = \eta - (\eta^2-1)^{1/2}. \end{cases} \tag{5.9}$$

The variations of phase ψ' given by (5.8) are represented in Fig. 4. The variations of the phase ψ of ξ are easily deduced from those of ψ' by a translation equal to the phase φ_h of the structure factor (5.5) and therefore depend on the origin of the unit cell. They are summarized in Table 1.

Another way to represent the variation of the phase ψ is to represent the variation of the complex quantity ξ on the complex plane. This is done in Fig. 5.

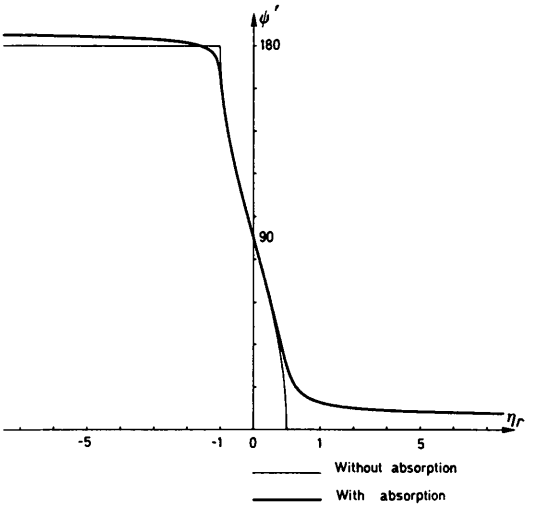

Fig. 4. Variation of the phase ψ' of $\eta \pm (\eta^2-1)^{1/2}$ in the absorbing and non-absorbing cases. Without absorption: $\psi' = \pi$ for $\eta \leq -1$; $\psi' = 0$ for $\eta \geq -1$. With absorption: the limits of ψ' are $\pi + \beta$ for $\eta_r \to -\infty$ and β for $\eta_r \to +\infty$ [β is the phase of $(F_h F_{\bar{h}})^{1/2}$]; ψ' is equal to π (the value in the non-absorbing case) for $\eta_r = -B/A$. In *both* cases, $\psi' = \pi/2$ for $\eta_r = 0$. The curves have been calculated for the case of a symmetric 111 reflection on a GaAs crystal for a wavelength $\lambda = 1{\cdot}195$ Å. For this example, $\beta = 6{\cdot}31°$, $B/A = 1{\cdot}58$.

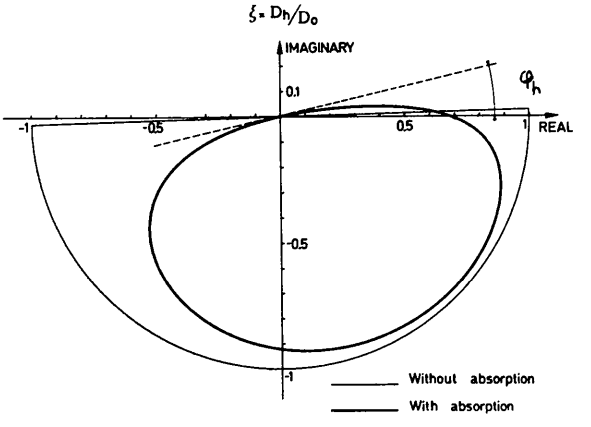

Fig. 5. Representation of the ratio, ξ, of the reflected to the incident amplitude in the complex plane in the absorbing and non-absorbing cases. The slope at the origin is equal to $\tan\varphi_h$, where φ_h is the phase angle of the structure factor, F_h. The curves for the absorbing and non-absorbing cases cross for $\eta_r = -B/A$. The example presented here has been calculated for a symmetrical 111 reflection on a GaAs crystal and $\lambda = 1{\cdot}195$ Å with the origin of the unit cell at mid-distance between gallium and arsenic planes. Such a representation was first used by Bonse (1964).

Table 1. *Variations of the phase and amplitude of the reflected wave in the non-absorbing case*

η	$-\infty$	-1	0	1	∞
ψ	$\pi+\varphi_h$	$\pi+\varphi_h$	$\pi/2+\varphi_h$	φ_h	φ_h
$\Delta d/d^*$	$-\varphi_h/2\pi$	$-\varphi_h/2\pi$	$0{\cdot}25-\varphi_h/2\pi$	$0{\cdot}5-\varphi_h/2\pi$	$0{\cdot}5-\varphi_h/2\pi$
$\lvert\xi\rvert$	0	1	1	1	0

* $\Delta d/d$ corresponds here to the position of the nodes in the unit cell.

5.4. *Reflecting power*

From (4.12) and (5.9), the reflecting power is equal to, in the three regions of the reflection domain,

$$\begin{cases} |\eta| \geq 1: & I_h = [|\eta| - (\eta^2-1)^{1/2}] \\ |\eta| \leq 1: & I_h = 1. \end{cases} \tag{5.10}$$

Equation (5.10) shows that there is total reflection for $|\eta| \leq 1$. This is the total reflection domain.

5.5. *Movement of the nodes of stationary waves when the crystal is rocked*

Expression (3.14) for the intensity of the wave field, (3.19), and Table 1 show that:

(*a*) The positions of the nodes and antinodes of the stationary waves are constant *outside the total reflection domain*;

On the small-angle side of the rocking curve ($\eta \leq -1$), the *nodes* lie on the planes where the phase φ_h of the structure factor F_h is equal to zero, that is on the planes for which the Fourier component of the electronic density is maximum.

On the large-angle side ($\eta \geq 1$), it is the *antinodes* which lie on these planes.

(*b*) Within the total reflection domain, the position of the nodes and antinodes *is displaced by $d/2$ towards the inside of the crystal* as the latter is rocked towards large angles of incidence (the normal to the crystal surface which corresponds to positive values of z is oriented towards the inside of the crystal).

The variation of the position of the nodes with the deviation parameter is represented in Fig. 6.

5.6. *Penetration depth–geometrical representation of the imaginary part of the wave vector within the total reflection domain*

The penetration depth in a non-absorbing crystal is finite within the total reflection domain only and is due to extinction. From (3.15), (3.13) and (5.9), it is

$$z_0 = -\gamma_0/(4\pi X_{0i}) = \Lambda/[2\pi(1-\eta^2)^{1/2}]. \tag{5.11}$$

The variations of z_0 can be visualized graphically by means of a new surface in reciprocal space which within the total reflection domain plays a role somewhat analogous to that of the dispersion surface outside. Equations (3.13) and (5.19) show that within the total reflection domain

$$K_{0i} = -i(1-\eta^2)^{1/2}/2\Lambda. \tag{5.12}$$

Equation (5.7) shows that outside the domain of total reflection $(\eta^2-1)^{1/2}$ is equal to the length of the chord of the dispersion surface intercepted by a line parallel to the crystal surface drawn from the extremity M of the incident wave vector and this can actually be taken as a geometric definition of the dispersion surface. In a similar way, one can consider in the plane of incidence the curve such that the chord intercepted by a parallel to the normal to the crystal surface should be equal to $(1-\eta^2)^{1/2}$. It is very easy to show that this is an ellipse tangent to the dispersion surface at I_1 and I_2 (Fig. 7). Let P_1 and P_2 be the intersections with this ellipse of the parallel to the normal to the crystal surface drawn from the extremity M of a wave vector within the total reflection domain; M_0 and M_h are the intersections of this normal with T_0 and T_h, respectively, as for a wave vector outside the total reflection domain. It can be shown that, in a similar way to (5.7),

$$\begin{cases} \eta = -\overline{M_0M_h}/\overline{I_{01}I_{h1}} \\ (1-\eta^2)^{1/2} = \overline{P_1P_2}/\overline{I_{01}I_{h1}} \end{cases} \tag{5.13}$$

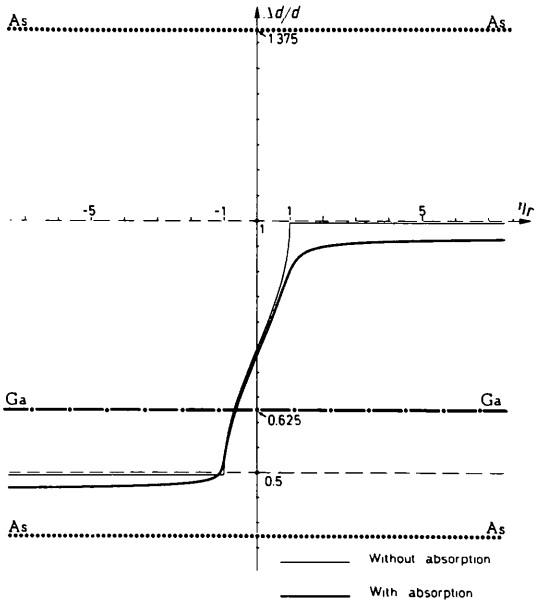

Fig. 6. Variations of the relative position of the nodes of stationary waves with the deviation parameter, η_r, with and without absorption. The curves have been calculated for a symmetrical 111 reflection on gallium arsenide and $\lambda = 1{\cdot}195$ Å. The thick dotted and dash-dotted lines show the positions of the arsenic and gallium (111) planes. The limiting position of the nodes far from the reflection domain in the non-absorbing case is slightly off the mid-distance between the arsenic and gallium planes. This is due to the difference between the form factors of gallium and arsenic. The change in the limiting position in the absorbing case should also be noticed. The ordinate axis is oriented towards the inside of the crystal from the surface.

and therefore, from (5.6),

$$z_0 = |2\pi \overline{P_1 P_2}|^{-1}. \tag{5.14}$$

The variation of the penetration depth is therefore given by that of the converse of the chord to the ellipse and its minimum value, reached at the middle of the total reflection domain, is equal to $\Lambda/2\pi$. Outside the total reflection domain, it is infinite. Fig. 8 represents the variations of z_0 with the deviation parameter within the total reflection domain.

6. Solution of the dynamical theory in the absorbing case

6.1. *Real and imaginary parts of the deviation parameter*

The index of refraction, the dielectric constant, the wave vectors and the dispersion surface are now complex. Furthermore, there is no longer a gap between the two branches of the dispersion surface and no total reflection. The geometric representation of the dispersion surface is no longer useful in the Bragg case, except outside the centre of the reflection domain, contrary to the Laue case. The reason is that the two main uses of the dispersion surface are firstly to give an idea of the variation of ξ with the deviation parameter and secondly to provide the propagation direction of the wave fields, which is normal to it at the tie point. In the absorbing Laue case, the imaginary parts are so small in general that the dispersion surface gives a good indication for these two purposes. In the Bragg case, where the imaginary parts are very large close to the total reflection domain, this is no longer true. The tangent of the angle of the propagation direction with the lattice planes is given in all cases by $[(1-|\xi|^2)/(1+|\xi|^2)]\tan\theta$ (von Laue, 1960) so that ξ is the main parameter and was used by Penning & Polder (1961) and Bonse (1964) for the study of wave-field propagation in slightly deformed crystals.

The deviation parameter is also complex and can be written:

$$\eta = \eta_r + i\eta_i \tag{6.1}$$

with

$$\begin{cases} \eta_r = [\Delta\theta \sin 2\theta \cos\beta + (1-\gamma)(\chi_{r0}\cos\beta \\ \qquad + \chi_{i0}\sin\beta)/2]/|C||\chi_h\chi_{\bar{h}}\gamma|^{1/2} \\ \quad = 2(\Delta\theta - \Delta\theta_0)/\delta \\ \eta_i = A\eta_r + B \\ A = -\tan\beta \\ B = [\chi_{i0}/(|C||\chi_h\chi_{\bar{h}}|^{1/2}\cos\beta)](1-\gamma)/2|\gamma|^{1/2}, \end{cases} \tag{6.2}$$

where β is defined by (2.5) and (2.7); A therefore depends on the 'h' Fourier coefficients of the real and imaginary parts of the dielectric susceptibility. γ defines the asymmetry of the reflection and was defined after (4.4). B is identical to the coefficient g defined by equation (3.181) of Zachariasen (1945), to the cos β factor.

When $\eta_r = -B/A$, $\eta_i = 0$, and many quantities are equal to their value in the non-absorbing case; this is the case for instance for the phase ψ' and for the amplitude Z of $\eta \pm (\eta^2-1)^{1/2}$.

In a centrosymmetric crystal with a small absorption and for a symmetric reflection ($\gamma = -1$), the parameters A and B reduce to

$$\begin{cases} A = -|\chi_{ih}/\chi_{rh}| = -\kappa \\ B = -|\chi_{i0}/C\chi_{rh}|. \end{cases} \tag{6.3}$$

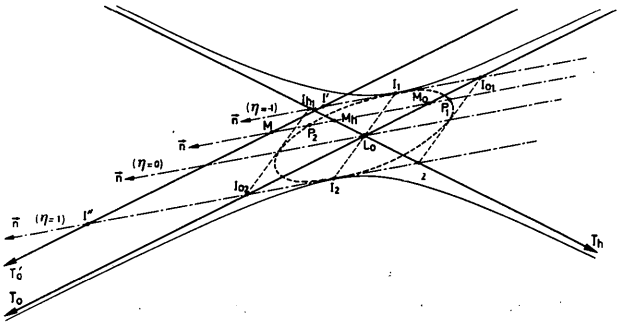

Fig. 7. Geometric interpretation in reciprocal space of the variations of the penetration depth in the case of a non-absorbing crystal. A new surface is introduced whose intersection with the plane of incidence is the ellipse drawn in dotted lines which is tangent to the dispersion surface at the extremities of the diameter I_1I_2 where the tangent is parallel to the crystal surface. The penetration depth z_0 is the converse of 2π times the chord P_1P_2 of the ellipse intercepted by the normal to the crystal surface drawn from the extremity M of the incident wave vector.

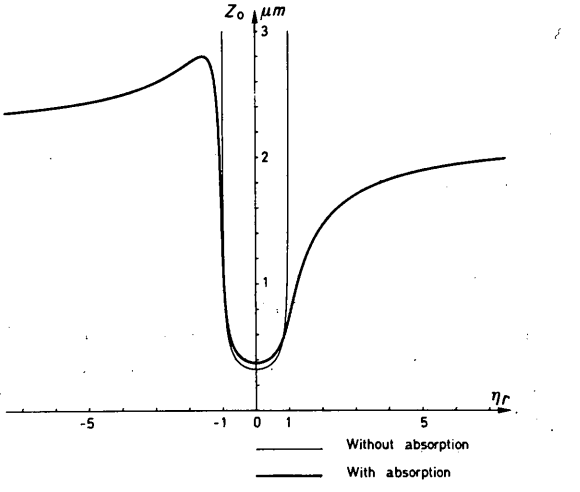

Fig. 8. Variation of the penetration depth with and without absorption. The curves have been calculated for a symmetrical 111 reflection on gallium arsenide for $\lambda = 1{\cdot}195$ Å.

Therefore, the ratio B/A which governs many of the properties of the wave fields is of the order of the ratio of the '0' and 'h' Fourier components of the imaginary parts of the susceptibility, χ.

The angle between the middle of the reflection domain and the geometrical Bragg angle, the width of the rocking curve and the real part of the extinction distance are now equal to, respectively,

$$\begin{cases} \Delta\theta_0 = -(1-\gamma)(\chi_{r0}+\chi_{i0}\tan\beta)/2\sin 2\theta \\ \delta = 2(\lambda/\Lambda_r)|\gamma_h|/\sin 2\theta \\ \Lambda_r = \lambda(\gamma_0|\gamma_h|)^{1/2}\cos\beta/|C||\chi_h\chi_{\bar{h}}|^{1/2}. \end{cases} \quad (6.4)$$

It should be noted that with the above definition the deviation parameter has the same sign as $(\Delta\theta - \Delta\theta_0)$ in both the Laue and the Bragg cases, contrary to the convention used by some other authors (for instance Zachariasen, 1945). It should also be noted that (6.4) show that the width of the rocking curve is absorption dependent.

6.2. *Reflecting power*

In order to calculate (4.12) for the reflecting power, we shall follow a derivation analogous to that of Fingerland (1971). The expression for the square of parameter Z defined in (4.8) can be written, when the deviation parameter is complex,

$$Z^2 = |\eta|^2 + \rho^2 + \eta * \rho \exp i\omega + \eta\rho \exp -i\omega. \quad (6.5)$$

We set

$$\begin{cases} L = |\eta|^2 + \rho^2 \\ M = \eta * \rho \exp i\omega + \eta\rho \exp -i\omega. \end{cases} \quad (6.6)$$

It can easily be shown that

$$\begin{cases} M = 2\rho(\eta_r \cos\omega + \eta_i \sin\omega) \\ M^2 = L^2 - 1 \end{cases} \quad (6.7)$$

and therefore that

$$Z^2 = L \pm (L^2-1)^{1/2}, \quad (6.8)$$

the solution to be chosen being, as mentioned earlier, that for which Z^2 converges. From (4.12) and (6.8), the reflecting power is

$$I_h = |\sigma|[L - (L^2-1)^{1/2}]. \quad (6.9)$$

This way of writing the Darwin-Prins formula was first used by Hirsch & Ramachandran (1950). There is no longer a total reflection domain and the rocking curve is asymmetric. Its properties are described in various papers (Hirsch & Ramachandran, 1950; Bucksch, Otto & Renninger, 1967; Fingerland, 1971). The shape of the curve depends through B and A on the '0' and 'h' Fourier components of the imaginary part of the dielectric susceptibility and on the asymmetry of the reflection. Its asymmetry decreases as B/A increases towards infinity for a given value of B. As shown by (6.2) and (6.3), this means that for given values of the normal absorption coefficient and of the asymmetry of the reflection, the asymmetry of the rocking curve decreases with the ratio $|\chi_{ih}/\chi_{i0}|$ of the 'h' to the '0' Fourier component. This is of course due to the anomalous absorption, or Borrmann effect, as will be discussed in § 6.4. For a given value of the '0' and 'h' Fourier components of absorption and therefore for a constant value of A, a change of the orientation of the reflecting planes with respect to the crystal surface induces a change in the values of B (6.2) and of B/A and therefore also a modification in the asymmetry of the rocking curve. On the other hand, the value of the maximum of the rocking curve decreases with increasing values of $|B|$ for constant values of B/A, that is it decreases with increasing absorption.

Far from the reflection domain, $\eta_r \to \pm\infty$, $L \to +\infty$ and, from (6.8),

$$Z^2 \to 1/2L. \quad (6.10)$$

6.3. *Phase of the reflected wave and its limits far from the reflection domain*

The phase angle ω is given by, from (4.8),

$$\begin{cases} \sin 2\omega = 2\eta_i\eta_r/\rho^2 \\ \cos 2\omega = (\eta_r^2 - \eta_i^2 - 1)/\rho^2, \end{cases} \quad (6.11)$$

the proper solution being, for the reason given above, that for which M [(6.6) and (6.7)] is positive. Using this value of ω, the phase angle ψ' is given by

$$\begin{cases} Z\cos\psi' = \eta_r + \rho\cos\omega \\ Z\sin\psi' = \eta_i + \rho\sin\omega. \end{cases} \quad (6.12)$$

Since there is now no total reflection domain, the phase angle of the reflected wave, $\psi = \psi' + \beta$ (4.10) now varies continuously and is no longer constant for $|\eta| \geq 1$. It is easy to show that $\psi' = \pi/2$ for $\eta_r = 0$ whatever the absorption as in the non-absorption case, and to π for $\eta_r = -B/A$ $(\eta_i = 0)$.

When $\eta_r \to \pm\infty$, $\eta_i \to A\eta_r$ and $\tan\omega \to A$. The condition mentioned above and (6.2) show that

$$\begin{cases} \omega \to -\beta & \text{for } \eta_r \to -\infty \\ \omega \to \pi - \beta & \text{for } \eta_r \to +\infty. \end{cases} \quad (6.13)$$

In order to calculate the limit of ψ', it is necessary to expand ω further. It is possible to show that when $\eta \to \pm\infty$

$$\begin{cases} \sin\omega \to -[\eta_i + A/2\eta_r(1+A^2)]/\rho \\ \cos\omega \to -[\eta_r - 1/2\eta_r(1+A^2)]/\rho \\ \rho \to |\eta_r|(1+A^2)^{1/2}[1+1/\eta_r(1+A^2)] \\ Z^{-1} \to 2|\eta_r|(1+A^2)^{1/2}[1+AB/2\eta_r(1+A^2)]. \end{cases} \quad (6.14)$$

From (6.13), (6.12) and (2.6), one deduces that

for $\eta \to -\infty$: $\psi' \to \pi + \beta$; $\psi \to \pi + \beta + \beta' = \pi + \varphi_h$

for $\eta \to \infty$: $\psi' \to \beta$; $\psi \to \beta + \beta' = \varphi_h$.

This very important result shows that the limits of the phase far from the reflection domain are expressed in the same way as in the non-absorbing case but including of course now anomalous dispersion and absorption in the calculation of the phase φ_h of the structure factor. This result was given independently by Authier (1985) and Bedzyk & Materlik (1985*b*). Table 2 summarizes the variations of the phase of the reflected wave for absorbing crystals.

Fig. 4 shows the variation of ψ' with η_r and Fig. 5 represents the variations of ξ in the complex plane.

6.4. *Anomalous absorption - shape of the rocking curve – penetration depth*

The effective absorption coefficient is given, using (3.17) and (4.9), by

$$\mu = \mu_0 + 2\pi k(\chi_h \chi_{\bar{h}})^{1/2} Z[\sin i(\beta + \psi')]/|\gamma|^{1/2}. \quad (6.15)$$

This is smaller than the normal absorption coefficient when $\psi' > \pi - \beta$. This occurs for values of η_r (see Fig. 4) corresponding to tie points lying on branch 1 of the dispersion surface which therefore, as in the Laue case, is associated with anomalously low absorption because the nodes of electric field coincide with the atomic planes. When $\psi' < \pi - \beta$, absorption is larger than normal. Within the Bragg gap, this is essentially due to extinction as shown in § 5.6; outside the Bragg gap, and for positive values of η_r, the tie points lie on branch 2 of the dispersion surface which is associated with anomalously high absorption because it is now the antinodes of the electric field which lie on the atomic planes. This is the Borrmann effect which is more explicitly understood in the case of transmission, or the Laue case; the expression for the effective absorption is given in that case and for a symmetric reflection [see, for instance, Authier, 1970, equation (II-6-4)] by

$$\mu = \mu_0[1 \mp |C|(\chi_{ih}/\chi_{i0})\cos\varphi/(1+\eta_r^2)^{1/2}], \quad (6.16)$$

where the minus sign corresponds to branch 1 and the plus sign to branch 2, φ is given by (2.5) and the deviation parameter is defined by (6.2) as in the Bragg case.

The advantage of the transmission case is that it is obvious from (6.16) that one branch of the dispersion surface correponds to anomalously high absorption and the other to anomalously low absorption. Furthermore, it is readily seen that the effect decreases with decreasing values of the ratio $|\chi_{ih}/\chi_{i0}|$, whatever the value of μ_0, as is very well known. It is the same effect that is at the origin of the asymmetry of the rocking curve in the Bragg case and of the influence of $|\chi_{ih}/\chi_{i0}|$ on this asymmetry, the influence that was noticed at the end of § 6.2: the left shoulder corresponds to wave fields with tie points on branch 1 with anomalously low absorption and the right shoulder to wave fields with tie points on branch 2, with anomalously high absorption.

The penetration depth z_0 in the Bragg case is given by (3.16) and (6.15); it varies continuously with η_r, contrary to the non-absorbing case and its variations are represented in Fig. 8 in the case of gallium arsenide. The asymmetry of the curve is of course due to the anomalous absorption effect just described.

7. Position of the nodes of stationary waves

7.1. *General results*

The variations of the positions of the nodes of stationary waves in the presence of absorption as the crystal is rocked through the reflection domain are summarized in Table 2 and illustrated in Figs. 6 and 9. It can be noticed that:

(*a*) *the position of the nodes is never constant*, contrary to the non-absorbing case; it is continuously moving towards the inside of the crystal as the latter is rocked towards large angles of incidence.

(*b*) the position of the nodes far from the reflection domain on the small-angle side lies on the planes

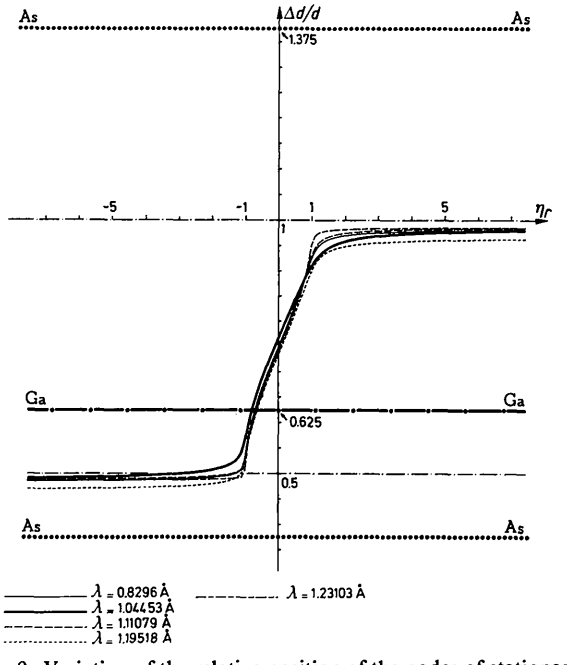

Fig. 9. Variation of the relative position of the nodes of stationary waves with the deviation parameter for various wavelengths. The curves were calculated for gallium arsenide, 111 reflection and the various wavelengths used by Bedzyk, Materlik & Kovalchuk (1984). The limiting position of the nodes far from the reflection domain depends on the wavelength. This is because of the difference in absorption. The thick dotted and dash-dotted lines represent the positions of the arsenic and gallium (111) planes and the ordinate axis is oriented towards the inside of the crystal.

Table 2. *Phase of the reflected wave and position of the nodes of stationary waves in the absorbing case*

η_r	$-\infty$	$-B/A$	0	∞
ω	$-\beta$	0	$\pi/2$	$\pi-\beta$
ψ'	$\pi+\beta$	π	$\pi/2$	β
ψ	$\pi+\varphi_h$	$\pi+\beta'$	$\pi/2+\beta'$	φ_h
$\Delta d/d$	$-\varphi_h/2\pi$	$-\beta'/2\pi$	$0{\cdot}25-\beta'/2\pi$	$0{\cdot}5-\varphi_h/2\pi$

Note that, in centrosymmetric crystals, the phase β' of $(F_h/F_{\bar{h}})^{1/2}$ is equal to zero when the origin is chosen at a centre of symmetry and that the phases φ_h of the structure factor and β of $(F_hF_{\bar{h}})^{1/2}$ are then equal.

where the phase φ_h of the structure factor is equal to zero, as in the non-absorbing case, but *this phase is now absorption dependent and so is the resulting shift of this position with respect to the limit determined in the non-absorbing case.* This absorption dependence of the limit exists both in centrosymmetric and non-centrosymmetric crystals. Far from the reflection domain on the large-angle side, the nodes lie on the planes where $\varphi_h+\pi$ is equal to zero. The total displacement of the nodes across the reflection domain is therefore equal to $d/2$, as in the non-absorbing case.

(*c*) *the position of the planes for a given value of the deviation parameter within the reflection domain is also absorption dependent,* in particular in the central part of the reflection domain for *non-centrosymmetric* crystals; this is shown very vividly in the example described in the next section. In centrosymmetric crystals, however, the phase, β', of $(F_h/F_{\bar{h}})^{1/2}$ is equal to zero when the origin is situated at a centre of symmetry and the position of the nodes at the middle of the reflection domain (close to $\eta_r=0$) is not absorption dependent; when the magnitude of the deviation parameter $|\eta_r|$ is close to 1 or larger, the position becomes strongly absorption dependent, as in non-centrosymmetric crystals.

7.2. *Example*: GaAs

7.2.1. *Structure factor.* Gallium arsenide has the zincblende structure; gallium lies at the nodes of a face-centred cubic lattice and arsenic occupies half the tetrahedral sites. The structure can be described as a compact packing $AA'BB'CC'$ of {111} planes occupied alternately by arsenic and gallium atoms, the distance of the A and A' planes being one third of that of the A' and B planes (see Figs. 6 and 9). The structure factor is

$$F_h=4[f_{Ga}\exp 2\pi i(h+k+l)/8 + f_{As}\exp -2\pi i(h+k+l)/8] \quad (7.1)$$

with the origin located at the mid-distance between a gallium and an arsenic atom along a [111] direction, that is at the mid-distance between an A' and a B plane.

For a 111 reflection, the structure factor is

$$F_{111}=-2\times 2^{1/2}[(f_{As}+f_{Ga})+i(f_{As}-f_{Ga})]. \quad (7.2)$$

Table 3. *Shifts of the position of the nodal planes for various wavelengths*: 111 *reflection on* GaAs

			$\eta_r=-\infty$		$\eta_r=0$	
λ(Å)	μ (μm^{-1})	$\lvert\sigma\rvert$	$\Delta d/d$	Δd (Å)	$\Delta d/d$	Δd (Å)
0·82096	0·048	0·985	−0·017	−0·055	−0·003	−0·010
1·04453	0·119	0·862	−0·014	−0·046	0·016	0·052
1·0450			Absorption edge of arsenic			
1·11079	0·054	1·118	−0·014	−0·046	−0·001	−0·004
1·19518	0·084	1·233	−0·034	−0·111	−0·016	−0·053
1·1958			Absorption edge of gallium			
1·23103	0·019	0·997	−0·016	−0·052	−0·010	−0·032
Non-absorbing case		1·000	−0·004	−0·014	−0·004	−0·014

The surface is then an arsenic plane with the normal oriented from the A towards the A' planes. It is the reverse for a $\bar{1}\bar{1}\bar{1}$ reflection which corresponds to a surface occupied by gallium atoms.

7.2.2. *Non-absorbing case.* In the non-absorbing case, the phase of the structure factor for 111 is

$$\varphi_h=\tan^{-1}[(f_{As}-f_{Ga})/(f_{As}+f_{Ga})] \quad (7.3)$$

and, since $f_{Ga}=26{\cdot}67$ and $f_{As}=28{\cdot}17$ for this reflection, it is readily seen that the position of the nodes is shifted by $\Delta d/d=0{\cdot}0044$ from the midpoint between the A, As, and A', Ga, planes towards the arsenic plane where the number of electrons is larger. This shift is of course due to the lack of a centre of symmetry and does not exist for germanium, for example. It is also directed towards the arsenic plane for the opposite reflection, $\bar{1}\bar{1}\bar{1}$.

7.2.3. *Absorbing case.* In the absorbing case, the phase of the structure factor for 111 becomes

$$\varphi_h=\tan^{-1}\left(\frac{f_{As}+f'_{As}+f''_{As}-f_{Ga}-f'_{Ga}+f''_{Ga}}{f_{As}+f'_{As}-f''_{As}+f_{Ga}+f'_{Ga}+f''_{Ga}}\right). \quad (7.4)$$

The phase of the structure factor for $\bar{1}\bar{1}\bar{1}$ is simply obtained by exchanging Ga and As in the above expression.

Fig. 6 compares the variations of the position of the nodes with the deviation parameter in the absorbing and non-absorbing cases for a 111 reflection and $\lambda=1{\cdot}195$ Å and Fig. 9 for the five wavelengths used by Bedzyk, Materlik & Kovalchuk (1984). These wavelengths correspond to energies lying on each side of the absorption edges of arsenic (1·0450 Å) and gallium (1·1958 Å). The corresponding values of the complex form factors were taken from the paper by Bedzyk *et al.* (1984). Table 3 gives the values of the relative and absolute shifts of the nodes from the position they would occupy in a centrosymmetric non-absorbing case for $\eta_r\to-\infty$ and $\eta_r=0$ for a 111 reflection and the wavelengths used in Fig. 9. The corresponding values of the absorption coefficient, μ, and of the departure from Friedel's law, $|\sigma|=|F_h/F_{\bar{h}}|$, are also given. Table 4 gives similar results for the opposite reflection, $\bar{1}\bar{1}\bar{1}$. It can be noticed that the

Table 4. *Shifts of the position of the nodal planes for various wavelengths:* $\bar{1}\bar{1}\bar{1}$ *reflection on* GaAs

The values of $\Delta d/d$ at $\eta_r = -\infty$ given in this table are identical with those given by Bedzyk & Materlik (1985*b*) for the 111 reflection (the convention for the orientation of [111] is different).

		$\eta_r = -\infty$		$\eta_r = 0$	
λ (Å)	$\lvert\sigma\rvert$	$\Delta d/d$	Δd (Å)	$\Delta d/d$	Δd (Å)
0·82096	1·015	−0·011	−0·035	−0·014	−0·045
1·04453	1·162	−0·046	−0·151	−0·030	−0·099
1·0450	Absorption edge of arsenic				
1·11079	0·895	−0·011	−0·036	−0·012	−0·040
1·19518	0·811	−0·001	−0·004	−0·017	−0·057
1·1958	Absorption edge of gallium				
1·23103	1·003	0·006	0·019	−0·004	−0·013
Non-absorbing case	1·000	0·004	0·014	0·004	0·014

shifts vary very strongly with absorption, the angular position of the crystal and the sense of the reflection. These absorption-dependent shifts are practically all negative, that is *directed towards the crystal surface*, for both the 111 and the $\bar{1}\bar{1}\bar{1}$ reflections, in other words, irrespective of whether the surface is an arsenic or a gallium plane. For comparison, in the case of germanium, which is centrosymmetric, the relative absorption-induced shift of the nodes far from the reflection domain is equal to 0.01 *towards the crystal surface* for a 111 reflection and $\lambda = 0{\cdot}709$ Å.

8. Concluding remarks

It has been shown in this paper that the position of the nodes of stationary waves is absorption dependent and varies continuously even outside the total reflection domain. Its limiting position far from the reflection domain has been determined; it is given simply by the phase of the structure factor, taking into account the imaginary parts of the form factors and anomalous dispersion. The relative absorption-induced shifts can be up to a few percent. In non-centrosymmetric crystals they affect the position of the nodes not only far from the reflection domain but also in the central part. These shifts are in general towards the crystal surface, irrespective of the sense of the diffraction vector.

A new surface has been introduced in reciprocal space which is tangent to the dynamical surface along parallels to the normal to the crystal surface, which enables a geometric representation to be given of the properties of wave fields in the total reflection domain where, as is well known, they are complex. In particular, this surface gives the imaginary part of the wave vectors and, therefore, the variation of the penetration depth. It is only valid, however, in the non-absorbing case. In the absorbing case, where there is no Bragg gap and the dispersion surface is complex with no discontinuity in its real and imaginary parts, there does not seem to be much use in its actual representation, except far from the total reflection domain.

The main properties of the various quantities used in dynamical theory, in particular for the standing-waves application, now seem well understood, in all their details, for the perfect absorbing crystal case. There are, however, situations occurring in practice of importance for interface investigations where further studies of the properties of standing waves seem required. This is the case, among others, for thin crystals where two wave fields have to be taken into account, for the presence of crystal imperfections which modify the propagation of wave fields inside the crystal and for steps on the crystal surface which may influence the application of the boundary limits or introduce diffraction effects. On the latter point a comment by von Laue (1960) may well be remembered, where he mentions that the approximation of a mathematical plane for the boundary limits is a 'better than nothing else' one justified by the agreement between experimental and theoretical rocking curves in the Bragg case but that it remains the 'weakest point in the dynamical theory'. The eventual influence of steps on the crystal surface should therefore be investigated.

Stimulating discussions with Dr J. R. Patel are gratefully acknowledged.

References

AFANAS'YEF, A. M., IMAMOV, R. M., MASLOV, A. V. & PAISHAYEV, E. M. (1985). *Kristallografiya*, **30**, 67–71.

AUTHIER, A. (1961). *Bull. Soc. Fr. Minéral. Cristallogr.* **84**, 51–89.

AUTHIER, A. (1970). *Advances in Structure Research by Diffraction Methods*, Vol. 3, edited by R. BRILL & R. MASON, pp. 1–51. Braunschweig: Vieweg.

AUTHIER, A. (1985). Ninth Eur. Crystallogr. Meet., Abstract 1-009.

BATTERMAN, B. W. (1964). *Phys. Rev.* **133**, a759–a764.

BATTERMAN, B. W. (1969). *Phys. Rev. Lett.* **22**, 703–705.

BATTERMAN, B. W. & COLE, H. (1964). *Rev. Mod. Phys.* **36**, 681.

BEDZYK, M. J. & MATERLIK, G. (1985*a*). *Phys. Rev. B*, **31**, 4110–4112.

BEDZYK, M. J. & MATERLIK, G. (1985*b*). *Phys. Rev. B*, **32**, 6456–6463.

BEDZYK, M. J., MATERLIK, G. & KOVALCHUK, M. V. (1984). *Phys. Rev. B*, **30**, 2453–2461.

BONSE, U. (1964). *Z. Phys.* **177**, 385–423.

BUCKSCH, R., OTTO, J. & RENNINGER, M. (1967). *Acta Cryst.* A**23**, 507–511.

DURBIN, S. M., BERMAN, L. E., BATTERMAN, B. W. & BLAKELY, J. M. (1986). *Phys. Rev. Lett.* **56**, 236–239.

EWALD, P. P. (1917). *Ann. Phys. (Leipzig)*, **54**, 519–597.

EWALD, P. P. (1927). *Handbuch der Physik*, Vol. 24, pp. 254–262. Geiger u. Scheel: Springer.

FINGERLAND, A. (1971). *Acta Cryst.* A**27**, 280–284.

GOLOVCHENKO, J. A., PATEL, J. R., KAPLAN, D. R., COWAN, P. L. & BEDZYK, M. J. (1982). *Phys. Rev. Lett.* **49**, 560–563.

HIRSCH, P. B. & RAMACHANDRAN, G. N. (1950). *Acta Cryst.* **3**, 187–194.

JAMES, R. W. (1963). *The Dynamical Theory of X-ray Diffraction.* In *Solid State Physics*, edited by F. SEITZ & D. TURNBULL, Vol. 15, p. 53. New York: Academic.

KATO, N. (1974). In *X-ray Diffraction*, by L. V. AZAROFF, R. KAPLOW, N. KATO, R. J. WEISS, A. J. C. WILSON & R. A. YOUNG, chs. 3, 4 and 5. New York: McGraw-Hill.

KRUGLOV, M. V., SOZONTOV, E. A., SHCHEMELEV, V. N. & ZAKHAROV, B. G. (1977). *Kristallografiya*, **22**, 693-697.

LAUE, M. VON (1931). *Ergeb. Exakten Naturwiss.* **10**, 133-458.

LAUE, M. VON (1960). *Rontgenstrahl Interferenzen.* Frankfurt am Main: Akademische Verlagsgesellshaft.

PATEL, J. R. & GOLOVCHENKO, J. A. (1983). *Phys. Rev. Lett.* **50**, 1858-1861.

PATEL, J. R., GOLOVCHENKO, J. A., BEAN, J. C. & MORRIS, R. J. (1985). *Phys. Rev. B*, **31**, 6884-6886.

PENNING, P. & POLDER, D. (1961). *Philips Res. Rep.* **16**, 419-440.

PINSKER, Z. G. (1978). *Dynamical Scattering of X-rays in Crystals.* Berlin: Springer.

TAKAHASHI, T. & KIKUTA, S. (1979). *J. Phys. Soc. Jpn*, **47**, 620.

ZACHARIASEN, W. H. (1945). *Theory of X-ray Diffraction in Crystals.* New York: John Wiley.

Acta Cryst. (1986). A**42**, 426-435

The Dynamical Diffraction of X-ray Spherical Waves in Two Perfect Crystals

BY V. V. ARISTOV AND A. A. SNIGIREV

Institute of Problems of Microelectronic Technology and Superpure Materials, USSR Academy of Sciences, 142432 Chernogolovka, Moscow District, USSR

AND A. M. AFANAS'EV, V. G. KOHN AND V. I. POLOVINKINA

I. V. Kurchatov Institute of Atomic Energy, Moscow 123183, USSR

(*Received* 22 *August* 1985; *accepted* 10 *February* 1986)

Abstract

The general theory of X-ray spherical-wave diffraction in two, either identical or different in nature, spatially separated perfect crystals is developed. The theory takes into account the phase shift of the waves both inside the crystals and in vacuum before, between and after the crystals. The nonmonochromaticity of radiation, the source dimension and the placing of a slit before the first crystal are considered. The results of theoretical calculation and an experimental study of the interference fringes and focusing the radiation are presented. A good agreement between the experimental and theoretical data is obtained for values of the experimental parameters that affect focusing.

1. Introduction

The diffraction pattern on the film behind a perfect crystal due to X-ray-spherical-wave diffraction is known (Afanas'ev & Kohn, 1977) to be defined to a great extent by the wave phase change occurring both inside the crystal and in vacuum along the source-crystal-film wave path L. In other words, the form of the diffraction pattern depends on the parameter t/L, where t is the crystal thickness. To observe this dependence experimentally one has to use either monochromatic radiation (Aristov, Ishikawa, Kikuta & Polovinkina, 1981) or a special set-up in which polychromatic focusing is realized (Aristov, Polovinkina, Shmyt'ko & Shulakov, 1978; Kozmik & Mikhailyuk, 1978*a*, *b*; Aristov & Polovinkina, 1978; Aristov, Polovinkina, Afanas'ev & Kohn, 1980). In the above papers all the new details of the diffraction pattern introduced by the theory have been obtained experimentally, namely, focusing of the radiation and the anomalous form of the *Pendellösung* fringes.

The effect of an entrance slit placed in front of the crystal on the diffraction pattern has been investigated in the papers by Aristov, Kohn & Polovinkina (1980) and Aristov, Kohn, Polovinkina & Snigirev (1982). The slit was shown to play the role of an incoherent source when its width $2a$ is much less than either the source dimensions or the 'spectral' width $d_s = (\Gamma/\omega)L_1 \tan\theta_B$, where Γ is the half-width of the spectral line, ω is the radiation frequency, L_1 is the source-to-crystal distance and θ_B is the Bragg angle. This case is realized in standard section topography of the experimental set-up with a narrow slit before the crystal, which is equivalent to the case of a point source on the entrance surface of a crystal (Kato, 1961, 1968).

The present paper is related to a further study of the role of the vacuum in X-ray-spherical-wave diffraction. The Laue diffraction in two perfect crystals has been considered. It is particularly interesting owing to strong focusing occurring in two-block crystals with equal block thickness and $L = 0$. This effect was first seen in the case of a small gap between two identical crystals (Kato, Usami & Katagawa, 1967; Authier, Milne & Sauvage, 1968) when direct and diffracted beams were not spatially separated. In the first paper the stacking fault was used as a gap. The next step was made by Indenbom, Slobodetsky & Truni (1974). The effect was shown to occur also with a large gap between the blocks in the twice-reflected

0108-7673/86/060426-10$01.50